PHYSICO-CHEMICAL AND COMPUTER SIMULATION STUDIES OF THE ROLE OF CATION COORDINATION NUMBERS ON MELT PHYSICAL PROPERTIES

C. A. Angell, I. M. Hodge* and P. A. Cheeseman
Department of Chemistry, Purdue University, West Lafayette, Ind. 47907

Abstract.

Some cohesion-and ion mobility-related physical properties have been measured for binary molten salt systems in which a great disparity exists between the coordinating abilities of the two cations. The disparity, which is obtained by mixing small and/or highly charged inorganic cations with large singly charged cations in common anion mixtures, allows the inorganic cation freedom to choose its coordination number. The result of principal interest is the great influence that the choice made has on the physical properties of the binary solution, particularly when the inorganic cation is trivalent. For four-coordination (MCl_4^- anion formation) the melt fluidities and ion mobilities increase with increasing MCl_3 content up to maximum values at 50 mole %. For six coordination (MCl_6^{3-} anion formation) melt fluidities drop steeply, with increasing MCl_3 content, the case of $CrCl_3$ solutions being outstanding.

The findings are interpreted using results from molecular dynamics calculations on single component systems of MX_2 and MX_4 stoichiometries in which the effective radius of the M species is varied to produce changes of M coordination number and related physical changes.

INTRODUCTION

Although spectroscopic and thermodynamic measurements have been used for a long time in attempts to establish the presence or otherwise of particular structural groupings ("complex ions") in molten salts, relatively little systematic attention has been paid to the effects that the particular coordination number adopted by the metal cation in such complexes may be expected to have on the melt physical properties. Our attention was drawn to the importance of the coordination number during a study of glass transition temperature vs. composition relations in binary salt systems which was initially expected to give information on the importance of covalent bonding in inorganic complex ions. It develops that the nature of the bonding is of secondary importance, and influences the melt properties to a major extent only if it tips the energetic balance in favor of one or another coordination number. The latter, which appears to be the most important property-determining factor, may equally well be determined by simple packing geometry requirements or by other electronic factors such as d orbital ligand field site stabilisation energies. The results of experimental studies on liquid cohesion indicated by the glass transition temperatures, and on ionic mobilities, indicated by electrical conductivities, will be described.

* Department of Chemistry, McGill Univ., Montreal, Canada (current).

To support the implications of the experimental studies we have turned to computer simulation studies, initially of single component melts. In these we use the molecular dynamics program of Woodcock (1) as modified by Woodcock, Angell and Cheeseman (2), in what may be termed the "modelling mode". In the "modelling mode" a system corresponding to an experimental substance, e.g. BeF_2, is modified by change of a single parameter in the pair potential function in order to explore the consequences to structure and properties of that parameter alone. In the present study we have followed the relaxation to new equilibrium structures of BeF_2- (2,3) and CCl_4 (4) -like liquids after changing the "repulsive potential size" parameter characterising the Be and C species. Again the property changes observed can be directly correlated with the changes in the coordination numbers of these two species.

In the experimental studies all measurements have been carried out on binary molten chloride systems containing a common component which has a low melting point, supercools readily, and functions as a good chloride ion donor. This combination of properties maximises the stability and definition of any complex groupings which form in the binary systems. The organic salt α-picolinium chloride (α-picHCl) was found an excellent choice for these purposes. This salt differs from the pyridinium chloride used in an earlier study of binary solutions with $ZnCl_2$ (5) only by the addition of a methyl group in the α ring position. The modification lowers the melting point considerably (from 143.5° to 89°C) and thereby confers very useful glassforming ability both on the pure salt and on wide composition ranges of its binary solutions.

Systems with such low-melting organic salts as one component provide an interesting class of binary salt solutions characterised by well-defined complex species in many cases and by very low liquidus temperatures. To illustrate their features, one system (α picolinium chloride + $AlCl_3$) has been characterised in some detail with respect to solid phases forming and liquid-solid phase relations. As seen below, such a system provides a range of "ambient temperature molten salts", some compositions in which remain liquid to well below 0°C.

EXPERIMENTAL SECTION

1. Laboratory Experiments.

Materials.

The salt α-picHCl was prepared in crude form by distilling water from a mixture of reagent grade concentrated hydrochloric acid (Mallinkrodt) and a small (~5%) excess of α-picoline (Aldrich). The salt was then distilled at 235°C and purified by sublimation. The product was a white, crystalline deliquescent material with a melting point of 89 ± 1°C (substantially above the value of ca 80°C quoted in Beilstein (6) from an 1899 reference). Microanalysis of the material gave the correct stoichiometry to within experimental error (±0.3% per determination). Although contamination by the β- and γ- isomers, or by N-methylpyridinium chloride would not be detected by microanalysis, the reproducibility of the melting point indicates that such contamination was probably small. To facilitate measurements of T_g the salt was prepared in the form of beads approximately 2 mm in diameter. This was accomplished with a specially designed sublimator which enabled the salt to be melted, drop by drop, into liquid nitrogen.

Glass Transition Temperatures.

Glass transition temperatures for the various solutions of α-picHCl + second components were determined by means of a simple differential thermal analysis technique using a sample cell (Fig. 1) which permitted stepwise additions to an initial solution of beads of organic salt which could be rolled through a side-arm from a storage vessel (see Fig. 1). Thus an entire binary system could be explored over its glassforming composition range without dismantling the cell and exposing its (usually hygroscopic) contents to the atmosphere. The sample cell, and a reference cell of the same dimensions containing anthracene, were seated in twin holes in an aluminum block.

Differential emfs observed during warmup at 10°min^{-1} from dry ice temperature by a Fig. 1b arrangement of Cr/Al thermocouples in thin pyrex glass sheaths (Fig. 1a), were recorded using a Honeywell Electronic 19 two pen recorder. T_g values, defined as shown by Fig. 1c, were reproducible to ±1°C, although T_g for α-picHCl itself was always observed to be -42.5 ± 0.5°C.

Electrical Conductance Measurements.

The conductance measurements were made with a Wayne-Kerr B221 impedance bridge, at an angular frequency of 10^4 rad sec^{-1}. Two types of cell were used, one similar to that described by Easteal and Angell (5) (cell constant 51.59) and the other the same as that used by Chin (7) (cell constant 74.33). The conductance cell was placed in an insulated aluminium block, which was heated by two Watlow cartridge heaters supplied through a Variac transformer. Most of the measurements were performed as the temperature slowly changed, the data being taken in this way agreeing with constant temperature data to within 0.5%. Agreement between different runs of pure α-picHCl was within ±0.5%, this large error being attributed to incipient decomposition. Most of the melts were a light to medium amber color at the end of a run.

Melt temperatures were determined with a glass-sheathed chromel-alumel thermocouple, the output of which was fed into a Hewlett-Packard 2212A VFC voltage-to-frequency converter and displayed digitally on a Dymec (now Hewlett-Packard) model 2801A quartz thermometer unit. The thermocouple was calibrated against the quartz thermometer over the temperature range 70-180°C. The rms deviation of the least squares quadratic calibration curve was 0.2°C, which is taken to be the accuracy of the temperature data. Both conductance cells were calibrated with 1 Demal potassium chloride solution at 25.00°C (8) and the cell constants are believed to be accurate to ±0.1%.

Density Measurements.

The density data were obtained using a dilatometer constructed by fusing a 1 ml pipette (graduated in 0.01 ml) to a 10 ml volumetric flask. The dilatometer was filled, and stoppered with a tube containing Drierite, in the drybox, removed, and immersed in a preheated silicone oil bath contained in a thermally insulated tube furnace. The reading error was ±0.002 ml (±0.02%). The dilatometer was calibrated with different quantities of water at two accurately determined temperatures (measured with the quartz thermometer), and the stem graduations were found to be accurate to within the reading error. The temperature was measured with a calibrated thermocouple placed in contact with the dilatometer bulb, using the same instruments described above for the conductance measurements. The bulb was placed in a region of minimum thermal gradient, measured as 0.1°C cm^{-1} vertically. The temperature data are believed to be accurate to within ±0.3°C and sensitive to within ±0.1°C. Readings were taken under equilibrium conditions (i.e. the temperature held constant until the volume was independent of time), since it was found that continuous heating or cooling techniques introduced systematic errors into the data. No correction for bulb expansion was applied because the expansion coefficient of pyrex glass is very much smaller than that of the melt.

Spectroscopic Measurements.

For certain solutions and compounds containing cations whose coordination numbers needed defining, Raman spectra and electronic spectra in the visible region were recorded. Raman spectra of room temperature samples were excited using a He-Ne laser and analysed using a Jarrel-Ash monochromator. The quality of liquid state Raman spectra of $CdCl_2$ and $ZnCl_2$ was poor due to a large background

probably from small quantities of organic decomposition products, but reasonable spectra of the crystallised materials were obtained. It is recognised that melt structures may be quite different from those of the corresponding crystals (9), but in view of the evidence from other Raman studies of $ZnCl_2$- and $CdCl_2$-containing fused chloride solutions (10,11), it is almost certain the Cd(II) and Zn(II) are similarly coordinated in each state.

Electronic spectra were obtained using a Cary 14R spectrophotometer with glassy or viscous liquid samples squeezed between glass plates.

2. Computer Simulation Experiments.

Ideally for the purposes of this paper it would be desirable to study, by computer simulation, the properties of binary systems containing a common cation and anion and a second cation whose effective radius in each system would be manipulated (by changing a single parameter in the appropriate pair interaction potential) in such a way as to make its coordination number different in each system. A suitable dynamics program, designed for computations on systems of arbitrary stoichiometries, has been developed but it has not been possible to utilise it for data production in time for this symposium. Fortunately, information sufficient to establish in most respects the significant connections between coordination numbers and physical properties with which this paper concerns itself is available from some preliminary runs on single component systems.

These calculations were carried out using a modified version of the program developed by Woodcock (1) for systems with charge-charge interactions and exponential repulsions.

The pair potential, utilised for this work, contained only Coulomb and exponential short range repulsion terms, as shown in Eq.(1).

$$\Phi_{ij}(r) = \frac{z_i z_j e^2}{r} + \left\{ 1 + \frac{z_i}{n_i} + \frac{z_j}{n_j} \right\} b \exp\left[(\sigma_i + \sigma_j - r_{ij})/\rho \right] \quad (1)$$

where z is the electronic charge, n is the number of outer shell electrons, σ is a distance parameter characteristic of the ionic radius, and b and ρ are constants. The parameters used were taken from Tosi and Fumi (12)(for Cl^-), and Busing (13)(for Be^{2+}, F^-), or else chosen arbitrarily to produce structural and related physical changes.

Programs were available for systems of MX_2 and MX_4 stoichiometries from previous work (2, 4). In this paper we report the changes in structure resulting from changing the value of the σ_+ parameter from values utilised in earlier simulations of structure and transport in BeF_2(2) and CCl_4(4). No explanation of the principle of MD simulations will be given here. The reader is referred to earlier

articles (14-16).

The simulation runs needed to demonstrate the effects of interest were quite short. Using an initial configuration from the equilibrated state of BeF_2, which is a four-coordinated network liquid, the program execution was continued after increasing the σ_+ parameter from 0.934 Å used for BeF_2 to 1.5 Å to increase the distance at which the ++ and +- pair repulsions begin to increase rapidly, i.e. to effectively increase the "size" of the cation. The calculation was carried out for 500 time steps of which the first 100 served to allow the program to disperse the excess initial repulsion energy and restore the original temperature. Because the final pressure was in excess of the initial pressure by ~100 kbar, a further 400 Δt were executed at a 20% increased volume, restoring the original pressure.

In the case of MX_4 liquids the σ_+ parameter was modified in both directions. Short separate runs, with σ_+ increased to 1.33 from 1.00 Å value used to simulate CCl_4, and also decreased to 0.90 and 0.70 Å, were carried out. In this case the changes in pressure, which were negative, were insufficient to warrant adjustments in the sample volume.

RESULTS

1. Laboratory Experiments.

The phase diagram derived for the α-picHCl + $AlCl_3$ system is shown in Fig. 1. In addition to the expected (α-picH) $AlCl_4$ compound, m.p. 83°C, a compound at 33.3% $AlCl_3$, (α-picH)$_2Al_2Cl_5$, with a slightly higher melting point, 85°C, is found. There is no counterpart to this compound in the familiar NaCl-$AlCl_3$ and KCl-$AlCl_3$ systems. No evidence for a crystalline compound (α-picH)Al_2Cl_7 was found, although the anion has been identified from melt spectra in the alkali halide-$AlCl_3$ systems (17,18). The deep eutectic, -19°C, between the (α-picH)$AlCl_4$ compound and $AlCl_3$, which may be associated with the absence of any such compound, is to be noted.

Glass transition temperatures, T_g, for the various α-picHCl + MCl_n solutions studied are plotted vs mol% MCl_n in Fig. 3. The range of the data indicate the extent of the glassforming composition region except in the cases of $CaCl_2$, $ZnCl_2$, $CrCl_3$, $FeCl_3$ and YCl_3. Except for MCl_3 additions, T_g always shows an initial increase, which becomes a weak maximum for those MCl_2 salts which are commonly believed to form MCl_4^{2-} anions. Although most systems with high $MXCl_2$ solubilities crystallise readily in the vicinity of the (α-picH)$_2$ MCl_4 stoichiometry (because of the relatively high melting point of the crystalline compound), it appears from the data on the $ZnCl_2$ system that T_g would pass through a weak minimum at the MCl_4^{2-} composition. In the case of $AlCl_3$ solutions, T_g shows evidence of a plateau in the $AlCl_4^-$ - $Al_2Cl_7^-$ stoichiometry range, though a minimum at $AlCl_4^-$ might have been anticipated from the behavior of $ZnCl_2$-based systems (Fig. 3 and ref. 5). The sharp increases in T_g with additions of salts of cations which do not form com-

pounds of MX_4^{n-} stoichiometries is to be noted, the case of α-picCl • $CrCl_3$ solutions being particularly striking. Mixtures of $PbCl_2$ • α-picHCl were glassforming but the glass transition could not be detected for reasons that remain unclear. A very small change in heat capacity at T_g is implied, though this is not expected for such a system. A 33% solution of $PbCl_2$ did form a glass indicating either that $PbCl_4^{2-}$ does not exist as an energetically favored configuration, or that the melting point of the compound containing it is very low. The former possibility seems more likely.

Electrical conductivity data for solutions in the LiCl, $ZnCl_2$ and $AlCl_3$ binary systems at three different temperatures are shown in Fig. 4. The pronounced maxima at the stoichiometries of MX_4^{n-} in the $AlCl_3$- and $ZnCl_2$-containing systems respectively are the features of interest. Tables of data for solutions of the plotted compositions covering the temperature range 90-200°C are available from the authors as supplementary material. The temperature dependence of the conductivity conformed approximately to the empirical VTF equation

$$\kappa = A \exp -B/(T-T_0) \qquad (2)$$

the standard deviation of ln κ for the best-fitting parameters being ~0.1%. However, in some cases, systematic deviations of this same magnitude (which will not be discussed here) were observed. Results of density measurements for the same three salts are presented in Fig. 5 after conversion to molar volumes. Also included in Fig. 5 are plots of the equivalent volume V_E, where V_E is defined to be consistent with the idea that complexation of the inorganic salts is complete, and that the charge contained in a mole of solution therefore derives solely from the pyridinium chloride component. Thus

$$V_E = M_E/\rho = [M_{(\alpha\text{-picHCl})} + [X/(1-X)]M_{(MCl_n)}]\ \rho^{-1} \qquad (3)$$

This is certainly the appropriate way to assess the equivalent volume of $AlCl_3$ solutions for the purposes of evaluating their equivalent conductances, since pure $AlCl_3$ is a non-conducting molecular liquid. It is also reasonable for the solutions containing the strong Lewis acid $ZnCl_2$, but it is probably inappropriate for LiCl solutions in which complex ions are not normally expected. The equivalent volume defined by Eq. (1) is always larger by the factor $(1-X)^{-1}$ than the conventional fused salt solution equivalent volume, defined by

$$V_E = M_E/\rho = (1-X)M_{(\alpha\text{-picHCl})} + XM_{(MCl_n)} \qquad (4)$$

Values of the latter V_E are included in Fig. 4 for the case of LiCl solutions. Also shown in Fig. 4 are the expansion coefficients $\frac{1}{V}(\partial V/\partial T)_p$ for melts in these systems.

Raman spectra of crystalline $ZnCl_2$- and $CdCl_2$-containing salts are contrasted with the higher frequency part of the Raman spectrum of α-picHCl itself in Fig. 6a. Band positions assigned to the symmetric

stretch of the $ZnCl_4^{2-}$ and $CdCl_4^{2-}$ group in fused KCl solutions (17,20) (usually referred to as an "internal" mode of the complex), are shown by bars. The $ZnCl_4^{2-}$ and $CdCl_4^{2-}$ bands are displaced slightly to higher frequencies in the α-picH$^+$ salts because α-picH$^+$ is a weak counter-cation compared with K^+. The α-picHCl lattice mode is markedly displaced, to lower energy, because of the replacement of the Cl^- ions of the α-picHCl lattice with weakly attracting MCl_4^{2-} ions.

The electronic spectrum of Cr(III) in these melts is shown in Fig. 6b. It is readily identified from the spectra of known crystals as due to Cr(III) in six-fold octahedral coordination, this being strongly favored over four-coordination by the d^3 electronic configuration (19). The vertical lines indicate the maxima of bands assigned by Gruen and McBeth (20) to $CrCl_6^{3-}$ groups in dilute solutions of $CrCl_3$ in LiCl-KCl melts at higher temperature.

The electronic spectrum of dilute $NiCl_2$ in α-picHCl is already known (21,22). Ni(II) is tetrahedrally coordinated except under very high (~10 kbar) pressures (21). It may be assumed, on the basis of the deep blue color of the melts (24), that Ni(II) remains tetrahedrally coordinated in the concentrated solutions of Fig. 3.

2. Computer Simulation Experiments.

Results of the MD simulations are presented in Figs. 7 and 8, which compare the radial distribution functions, normalised to unity for large distances, for the different pair potentials (which differ only in the value of σ_+). The coordination number, obtained from the area under the first peak in the RDF, is indicated in each case. Included in Fig. 7 is an insert which indicates the time scale on which the adjustment to the new parameter occurs. The insert shows the variation with time of all species within 3.0 Å of a randomly chosen Be after it becomes instantaneously (at t=0) a M(σ_+=1.50) species. The temperature jumps instantaneously to 8000°K as the repulsive energy produced by the parameter change is converted into kinetic energy, but is returned to 1000K within 100 time steps by scaling down the particle velocities at each time step. In the same number of time steps the near neighbor distances increase from 1.57 to 2.4 Å and new near neighbors arrive from former second nearest neighbor anion positions to increase the coordination number to ~8 (within 2.8 Å).

In Table 1 additional data indicating the pressure of each system at the same volume, and the particle mobilities within that volume, are presented. Because of the shortness of the runs, these data are strictly of qualitative character, intended only to indicate the trend of the system's properties in response to the parameter changes.

DISCUSSION

The complex species $AlCl_4^-$ (17,18,24), $FeCl_4^-$ (25), $ZnCl_4^{2-}$(11),

$CoCl_4^{2-}$ (18) and $MgCl_4^{2-}$ (26), have been convincingly demonstrated to exist as geometric species in a variety of conventional molten salt systems. Their continued existence in the present systems is hardly to be doubted and, in view of the relatively unimportant counter-cation competition and very low melt temperatures, they can probably be assumed to be kinetically stable or "permanent" anions. Therefore, in view of the classical argument (27) that conductance decreases, and even conductance minima, should accompany the formation of complex ions in fused salt media, the finding in our work of pronounced maxima in conductance at complex ion stoichiometries is quite striking. It is clear from this observation that removal of added conducting species by complex formation, even if it does reduce the number of mobile ions per cc (which is by no means as axiomatic as in aqueous solutions) is insufficient to determine the conductivity behavior. Some other factor, which we will identify as the ionic mobility as distinct from its number density, must play a controlling role.

Ionic mobilities in fused salts generally scale with the melt fluidity (except near T_g)(28). Thus, the existence of conductivity maxima could be the result of ionic mobility associated with fluidity maxima (or viscosity minima). These in turn would be reflected in minima for isoviscosity temperature vs composition plots of which the T_g ($n \sim 10^{13}$ cp) vs composition plots in Fig. 3 provide examples. On this basis, the data of Fig. 3 show* that, in the cases of $AlCl_3$ and LiCl, changes in conductance with composition can be attributed primarily to changes in ionic mobilities which accompany inorganic chloride additions. Although Fig. 3 would imply initial decreases in conductance of the $ZnCl_2$ solutions which are not observed, the behavior of T_g at mole fractions of $ZnCl_2$ greater than 0.2 does imply a maximum in isothermal fluidity at the composition $(\alpha\text{-picHCl})_2ZnCl_4$ which means mobility changes would account for the conductivity maximum observed at this composition at higher temperatures. On the other hand for $AlCl_3$ solutions, the T_g plots indicate only a sudden change of composition dependence at the $AlCl_4^-$ stoichiometry rather than a fluidity maximum to correlate with the conductance maximum of Fig. 4. Of course the isothermal fluidity predictions based on Fig. 3 are only reliable for very low temperatures, and it may well be that at the temperatures of the conductance isotherms actual maxima in the fluidity isotherms would also be observed. The necessary direct measurements have yet to be made. In support of this possibility we note that the conductance maxima themselves become less pronounced with decreasing isotherm temperature, particularly when the specific conductance isotherms are converted to equivalent conductance isotherms using the V_E data of Fig. 5(a), see e.g. Fig. 4 for $AlCl_3$ solutions.

According to Fig. 3, the increases in conductance with added in-

* In simple cases of glassforming liquids, an argument by Angell (29) suggests that linear changes of glass temperature should produce exponential changes in the fluidity ϕ,

$$\phi = \phi_0 \exp - B/(X_0 - X)$$

organic salt would be even more striking for $FeCl_3$ solutions. It is of particular interest therefore that just the opposite behavior is predicted by Fig. 3 for behavior of systems containing $CrCl_3$, whose cation is only two protons (and two neutrons) removed from Fe^{3+} on the periodic table. The difference in these solution properties quite clearly lies in the difference in coordination number adopted by the added cation. Fe(III)(like Al(III)) always occurs as the tetrahedral $FeCl_4^-$ complex, while Cr(III), despite its comparable cation size, chooses 6 coordination, see Fig. 6(b). (The d^3 electronic configuration of Cr(III) favors octahedral over tetrahedral coordination by $\sim$ 12 kcal/mole(19)). A similar coordination number-based explanation can be given for the increases in T_g associated with YCl_3 and $CaCl_2$ additions, although in these cases the origin of the higher coordination number adopted by the cation (28) lies in geometrical packing factors related to the larger cation sizes rather than to ligand field stabilisation energies.

A physical understanding of the connection evident between the mass transport properties and the coordination numbers can be obtained with the help of the computer simulation results. In the first place the fact that it is possible to simulate the structure and simple fluid character of CCl_4 with the ionic potentials employed in this work (4) shows that, when ion sizes permit the appropriate coordination numbers, charge screening of highly charged cations by a near neighbor shell of anions can be very effective. The pressure of simulated CCl_4 at the experimental molar volume, for instance, is almost zero within the ±1 kbar fluctuations in the virial from which it is calculated (14,16) indicating that the CCl_4 molecules exert no important electrostrictive forces on each other. A consequence is that the system is found to be in the freely diffusive liquid state at 300K ($D_{C_4^+} \sim 2\times10^{-5}cm^2sec^{-1}$(4)). In like manner when M^{3+} cations form large MX_4^- anions from a matrix of Cl^-, the M^{3+} charge is screened out and a decrease in electrostrictive "pressure" follows. Under normal pressures, therefore, the system will occupy a large volume relative to that of a mixture of ionic quasi-lattices, indicated in Fig. 5 by the join between the $AlCl_3$ ionic crystal volume and the volume of molten α-picHCl. With the extra volume per mole of ions thus provided, all ionic mobilities increase. Such effects have been predicted for the case of charge cancellation by covalent bond formation (29), though we now see that the covalent bond per se is unnecessary (though the difference between $FeCl_3$ and $AlCl_3$ plots in Fig.3 may be due to the greater covalent character of the Fe-Cl bond).

To understand the contrary decrease in mobilities (or increase in T_g) when higher coordination numbers occur, one can point to the large residual unbalanced charge per complex ion and the consequent volume-constricting attractive interactions between these anions and their companion cations. Unfortunately no experimental measurements were made in this study of V_M for the six-coordinating systems to establish the contrast in volumetric behavior. Again however the simulation results are helpful. Fig. 8 and Table 1 show that when $\sigma_{M^{4+}}$ was increased, the coordination number of M^{4+} changed to $\sim$6 and the volume of the system "wanted" to decrease, because the pressure at the constant volume of

of the computation went to large negative values. This latter apparently contradictory response to increase in cation size is clearly a consequence of the increase in coordination number and the fact that the cations are now "tied together" through anion bridges (i.e. a network liquid rather than a molecular liquid exists). This has the further consequence that, even without allowing the volume to decrease to restore the original pressure, the average mean square displacemnt of the ions (over 300 time steps) decreases below the "CCl_4" value, Table 1. Such bridging of anions will also occur in, for instance, α-picHCl + $CrCl_3$ solutions at $CrCl_3$ concentrations of greater than 25 mol%, i.e. $(\alpha\text{-picH})_3 \cdot CrCl_6$.

The increases in T_g which occur even in dilute solutions, however, can be better understood in terms of the decrease in liquid configurational entropy which follows any $CrCl_3$ addition to α-picHCl. In the formation of $CrCl_6^{3-}$ by the addition of $CrCl_3$ to α-picHCl, each Cr^{3+} cation added to the melt immobilises three previously free Cl^- ions, converting the configurational degrees of freedom into entropy-poor internal vibrational degrees of freedom. The formation of $AlCl_4^-$ or $FeCl_4^-$, on the other hand, removes only one otherwise free Cl^-. Clearly the configurational entropy of the former solution will decrease relative to that of the latter as X_{MCl_3} is increased. Many authors have drawn attention to the close relation between the configurational entropy of glassforming liquids and their mass transport or relaxational properties. Such relations have been demonstrated (i) by the almost universal validity of the second Davies-Jones equation (30) for the pressure dependence of T_g (31)(which depends on the configurational entropy being constant at T_g),(ii) by the correlation of T_o of Eq. (2) for many pure substances with the configurational entropy zero point extrapolated from thermodynamic data (32,33), and (iii) by theoretical studies (34). The coordination number of a cation in a binary mixture will therefore influence the mobility of that ion and also of its neighbors through its effect on the configurational entropy of the solution containing it.

These statements are believed valid for solutions of the type measured in this study. However they must be qualified for systems in which addition of the second component breaks down a pre-existing low entropy network structure. In such a case an increase in coordination number could occur in association with increased particle mobilities while remaining consistent with the entropy-mobility correlation. The MX_2 simulation experiments provide a case in question. For $\sigma_{M^{2+}}$=0.934Å the tetrahedral network structure of BeF_2 is obtained, see Fig.7, and the diffusion coefficients are very small (3,4). After change of $\sigma_{M^{2+}}$ to 1.50, and an increase in volume to return the calculated pressure to its initial value, the mean square displacement after 400 time steps was found to be larger for both M^{2+} and F^- species than in the case of BeF_2, although the coordination number of M^{2+} had increased from 4 to 8(Fig.7).

Returning to the laboratory experiments, we note that the solutions in which the tetrahedral complexes of divalent cations are formed are intermediate in character between the [M(III)Cl_6] and [M(III)Cl_4] cases.

in the formation of M(II)Cl_4^{2-} group, two small singly charged anions are replaced by a large but (compensatingly) doubly charged anion, with a net loss to the solvent of only one "free" anionic species. With such competing influences, the outcome with respect to ion mobilities and T_g is uncertain, and is probably determined by the following factor not yet considered.

There is good evidence from proton magnetic resonance studies (35) that a strong association of α-picolinium cations can occur through hydrogen bonds to a bridging Cl^-. The congruently melting compound at 33% $AlCl_3$ (see Fig. 2) probably owes its existence to the stability of this bridged cationic species. These dimeric species are dissociated by removal of Cl^- by a strong Lewis acid (35). Such dissociation will commence around X=0.33 in MX_3 systems and around X=0.2 for MX_2 systems, and its dissociation will tend to increase the solution configurational entropy hence to lower T_g. It is probably responsible for the weak decrease in T_g beyond X=0.2 for MX_2 systems (Fig.3) and the particularly rapid decreases in T_g which must occur for X>0.4 in the $AlCl_3$ system (Fig.3). If such cationic complexes indeed play this complicating role, there would be advantages in repeating the present type of study using an organic salt in which the nitrogenic proton is replaced by a methyl group.

Concluding Remarks

Organic salts in general and those with inorganic anions in particular have been under-exploited in fused salt physical chemistry studies. Because of the greater definition of structure-related properties they permit, such salts deserve increased attention in both spectroscopic and classical experiments. Transport numbers of certain inorganic cations relative to the anion for instance should approach zero in some of these binary melts.

Acknowledgements

The authors are indebted to the National Science Foundation Grant DMR 73-02632 A01 and to the Purdue University NSF-MRL program for support of this research.

References.

1. L. V. Woodcock, Chem. Phys. Lett. 10, 257 (1971).
2. L. V. Woodcock, C.A. Angell and P.A. Cheeseman, J. Chem. Phys. (In press).
3. A. Rahman, R.H. Fowler and A.H. Narten, J. Chem. Phys. 57, 3010 (1972).
4. C. A. Angell and P.A. Cheeseman (to be published).
5. A. J. Easteal and C.A. Angell, J. Phys. Chem. 74, 3987 (1970).
6. Beilsteins Handbuch der Organischen Chemie, Band XX, p. 236.
7. D. Chin, Ph.D. Thesis, Purdue University, 1971.
8. G. Jones and B.C. Bradshaw, J. Am. Chem. Soc. 55, 1780 (1933).

9. M. A. Bredig in "Molten Salts--Characterization and Analysis" G. Mamantov, Ed., Marcel Dekker, N.Y. 1969.
10. J.H.R. Clarke and P.J. Hartley, J. Phys. Chem., 78, 595 (1974)
11.a) D.E. Irish and T.F. Young, J. Chem. Phys. 43, 1765 (1965).
b) P.B. Ellis, J. Electrochem. Soc. 113, 685 (1966).
c) W.E. Smith, J. Brynestad and G.P. Smith, J. Chem. Phys. 52, 3890 (1970).
12. F.G. Fumi and M.P. Tosi, J. Phys. Chem. Solids, 25, 31 (1964).
13. W.R. Busing, J. Chem. Phys. 57, 3008 (1972).
14. A. Rahman, Phys. Rev. 136, A405 (1964).
15. L. Verlet, Phys. Rev. 159, (1967).
16. L.V. Woodcock, Adv. Molten Salts, A Chemistry, Vol. 3, Chap. 1, pp. 1 - 75 (1975).
17. S. J. Cyvin, P. Klaboe, E. Rytter and H.A. Øye, J. Chem. Phys. 52, 2776 (1970).
18. C.R. Boxton, Adv. Molten Salt. Chem. 1, 176.
19. F.A. Cotton and G. Wilkinson "Advanced Inorganic Chemistry" Interscience Publ (1966), 2nd Ed. Ch. 26.
20. D.M. Gruen and R.L. McBeth, Pure Appl. Chem. 6, 23 (1963).
21. C.A. Angell and M.L. Abkemeier, Inorg Chem. 12, 1462 (1973).
22. M.L. Abkemeier, Ph.D. Thesis, Purdue University (1972).
23. I.M. Hodge, Ph. D. Thesis, Purdue University (1974).
24. B. Tremillon and G. Letisse, J. Electroaral. Chem. 17, 371 (1968).
25. A.P. Ginsberg and M.B. Robin, Inorg. Chem. 2, 817 (1963).
26.a) V. A. Maroni and E.J. Cairns, in "Molten Salts--Characterization and Analysis", G. Mamantov,Ed. Marcel Dekker, N.Y. 1969.
b) M.A. Bredig, in "Molten Salts--Characterization and Analysis" G. Mamantov, Ed., Marcel Dekker, N.Y. 1969.
c) J.H.R. Clarke and P.J. Hartley, J. Phys. Chem. 78, 595 (1974).
27. H. Bloom and E. Heymann, Proc. Roy. Soc. A 188, 392 (1947).
28. G. Papatheodorou (private communication of Raman Spectroscopy results on trivalent metal chloride + KCl solutions currently being prepared for publication.)
29. C.A. Angell, J. Phys. Chem. 70, 3988 (1966).
30. R.O. Davies and G.O. Jones, Adv. Phys. 2, 370 (1953); Proc. Roy. Soc. (London) A217, 26 (1953).
31 J.M. O'Reilly, J. Polymer Sci. 57, 429 (1962).
32. C.A. Angell and K.J. Rao, J. Chem. Phys. 57, 470 (1974).
33. C.A. Angell and J.C. Tucker, J.Phys. Chem. 78, 278 (1974).
34. G. Adam and J.H. Gibbs, J. Chem. Phys. 43, 139 (1965).
35. J.W. Shuppert, Ph. D. Thesis, Purdue University, 1974.

Table 1. Properties of Simulated MX_4 Liquids at V = 96.95 cm^3, T = 300±10

σ_M4+ (Å)	0.7	0.9	1.00	1.33
1. Thermodynamic Properties. a) P_{av}(kbar) over final 100 Δt	-2.1±1	-1.6±.1	-1.8±.5	-9.2±1
b) 10^{-6}E (kJ/mole) average over final 100 Δt	9.22	8.64	8.33	7.38
2. Structural Properties. a)RDF first peak position $r_{g(max)}$ (Å)	1.3	1.7	1.77	2.3
b)RDF first peak height g(max).	19.16	23.08	41.6	10.1
)Coordination number, N(r)[i] at $r_{g(max)}$	1.37	2.91		3.18
[i] at 0.1 $r_{g(max)}$	2.1	3.77		5.65
[iii]aat $r_{g(min)}$	4.96	4.01	4.000	5.8
[iv] comments. See below.	†	∇	*	†*
3. Transport Properties.				
$10^{16}t^2$ for C_M^{4+} after 300 Δt (Å²)	-	0.57	0.58	0.34

† 2 near neighbors off axis; 2 further making distorted tetrahedron

∇ Still molecular MX_4; some distortions since $\frac{r_{+-(max)}}{r_{--(max)}} = 1.65$

* Liquid of symmetrical tetrahedral molecules: $\frac{r_{+-(max)}}{r_{--(max)}} = 1.53$

†* Network liquid; many uniform 6's.

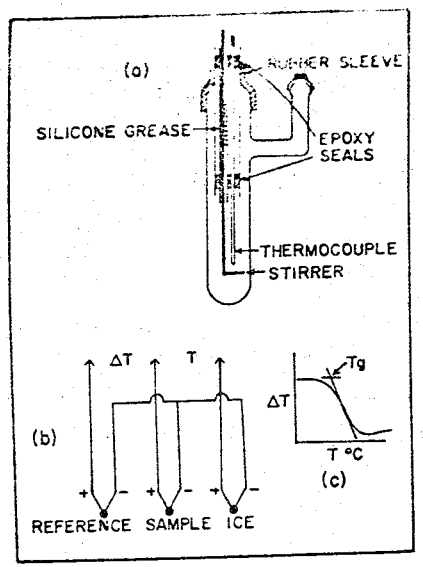

Figure 1 (a) Sample cell for DTA determinations of glass and phase transition temperatures. (b) Arrangement of sample and reference thermocouples for DTA studies. (c) Definition of T_g from differential emf vs temperature.

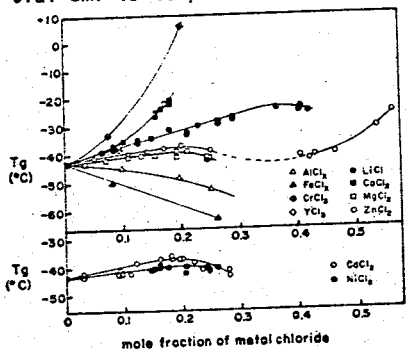

Figure 3. Glass transition temperatures for solutions of various inorganic chlorides in molten α-picolinium chloride.

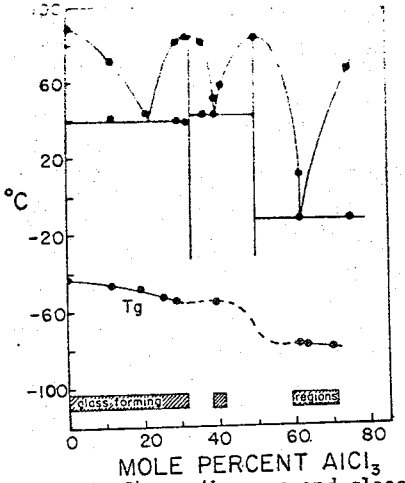

Figure 2. Phase diagrams and glass transition temperatures for the system α-picHCl + $AlCl_3$.

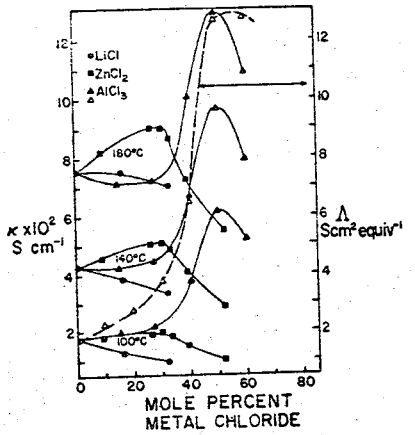

Figure 4. Specific conductivities for LiCl, $ZnCl_2$ and $AlCl_3$ solutions in α-picHCl at three temperatures, and the equivalent conductances of α-picHCl + $AlCl_3$ solutions at 100°C.

Figure 5. Molar volumes, equivalent volumes and expansion coefficients of α-picHCl + $AlCl_3$ solutions at 100°C. Data for pure salts are taken from the literature, using a long extrapolation into the supercooled state in the LiCl case.

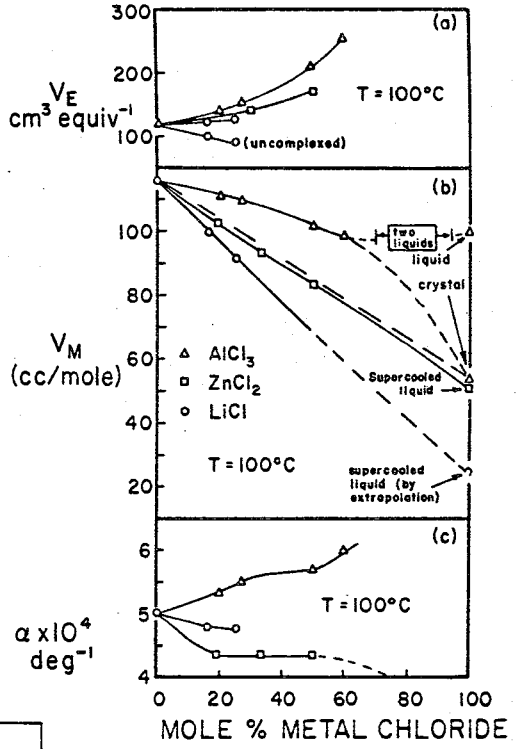

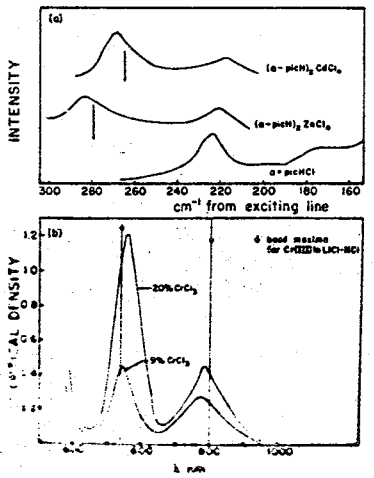

Figure 6. (a) Portions of the crystalline state Raman spectra of α-picolinium chloride, and its complex compounds with cadmium chloride and zinc chloride. (b) Visible and near IR spectra of Cr(III) in α-picHCl + $CrCl_3$ solutions of different concentrations demonstrating octahedral coordination of Cr(III) in these solutions. Shift in band maximum and increase in half width is attributed to distortions from octahedral symmetry due to Cr(III)-Cr(III) interactions (e.g. if some octahedra are chloride-bridged.

Figure 7. Individual pair distribution functions and M^{2+} coordination number N(f) for MF_2 liquids in cases
(a) $\sigma_+ = 0.934$ Å
(b) $\sigma_+ = 1.50$ Å
INSERT: Trajectories of all F^- neighbors around a randomly chosen M^{2+} species as a function of time before and after the change in σ_+ parameter.

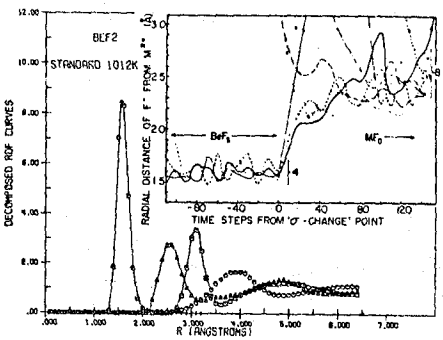

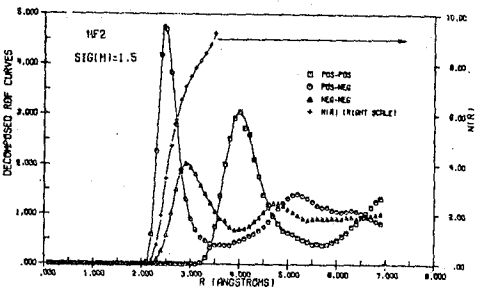

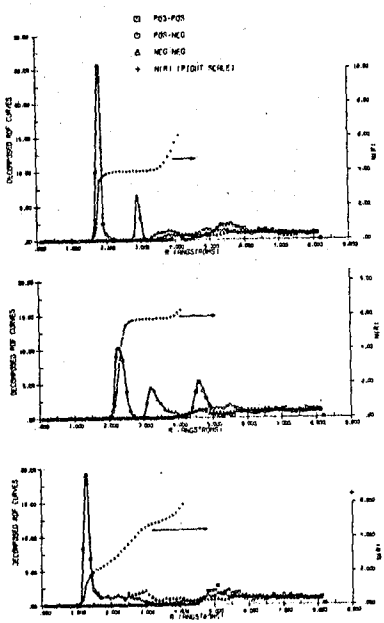

Figure 8. Individual pair distribution functions and M^{4+} coordination numbers N(r) for MCl_4 liquids for cases
(a) $\sigma_+ = 1.00$ Å
(b) $\sigma_+ = 1.33$ Å
(c) $\sigma_+ = 0.70$ Å
Note well-defined change in N(r) from 4.0 (molecular liquid) to ∿6.0 (network liquid) with change of σ_+ from 1.0 to 1.33 Å.